



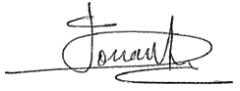


---

# EVALUATION OF THE MASS BALANCE OF ARCTIC GLACIERS WITH SATELLITE GRAVIMETRY MEASUREMENTS

---

## DESCRIPTION OF THE DATASET SUBMITTED TO THE GLACIER MASS BALANCE INTERCOMPARISON EXERCISE BY LEGOS - MAGELLIUM TEAM

	Name	Organisation	Date	Visa
<b>Written by:</b>	Julia Pfeffer Benjamin Coupry Etienne Berthier Alejandro Blazquez Anne Barnoud	Magellium Magellium LEGOS LEGOS / CNES Magellium	30/05/2023	
<b>Checked by:</b>	Julia Pfeffer	Magellium	30/05/2023	
<b>Approved by:</b>	Joël Dorandeu	Magellium	30/05/2023	

<b>Document reference:</b>	HYBRID_GRAVIMETRIE-DT-004-MAG_GLAMBIE_PUM
<b>Edition.Revision:</b>	1.0
<b>Date Issued:</b>	30/05/2023
<b>Customer:</b>	CNES

## Distribution List

	Name	Organisation	No. copies
Sent to :	GlaMBIE team	GlaMBIE	1

## Document evolution sheet

Ed.	Rev.	Date	Purpose evolution	Comments
1	0	30/05/2023	Creation of document	None

## Dissemination level

PU	Public	X
PP	Restricted to other programme participants	
RE	Restricted to a group specified by the consortium	
CO	Confidential, only for members of the consortium	

## Contents

<b>1 Introduction</b>	<b>3</b>
1.1 Overview	3
1.2 Document structure	3
1.3 References	4
1.4 Acronyms	7
<b>2 Study area and period</b>	<b>8</b>
<b>3 Data and Methods</b>	<b>10</b>
3.1 Overview	10
3.2 Global grids of surface mass anomalies	11
3.3 Regional glacier mass balances	14
<b>4 Results</b>	<b>15</b>
4.1 Total mass changes of Arctic glaciers regions	15
4.2 Hydrological contribution	18
<b>5 Product description</b>	<b>21</b>
5.1 File specifications	21
5.1.1 File format	21
5.1.2 File naming convention	21
5.1.3 Metadata	21
5.2 Variables	22

# 1 Introduction

---

## 1.1 Overview

This document describes the LEGOS-Magellium mass balance dataset for Arctic glaciers regions based on satellite gravimetry. The data product has been developed in collaboration between LEGOS and Magellium within the scope of the hybridation challenge funded by the CNES (R&T Hybrid Spatial Gravimetry 2022/2023).

The total mass balance is evaluated for five regions of the 6th version of the Randolph Glacier Inventory (RGI6, RGI Consortium, 2017), namely the Arctic Canada North, Arctic Canada South, Iceland, Svalbard and Russian Arctic. The total mass balance of Arctic glaciers is evaluated mainly based on satellite gravimetry measurements. An ensemble approach updated from Blazquez et al. (2018) is adopted to evaluate uncertainties associated with the processing and post-processing of GRACE (Gravity Recovery And Climate Experiment, Tapley et al., 2004) and GRACE-FO (GRACE-Follow On; Landerer et al., 2020) data. A priori information from DEM differencing (Hugonnet et al., 2021) is used to reduce leakage errors associated with the mislocation of signal sources. The effect of land hydrology is estimated for each region, but not corrected in the total mass balance dataset, because of the small water mass balance values and large errors inherent to hydrological models. Total mass changes expressed in Gt are estimated from April 2002 to September 2022 for five RGI regions. The uncertainty on total mass changes are provided with a confidence interval of 95%. The dataset is provided in the GlAMBIE CSV file format.

## 1.2 Document structure

---

The following document is organized as follows:

- Section 2 describes the study area and period,
- Section 3 summarizes the data and methodology,
- Section 4 provides a brief overview of the data content,
- Section 5 describes the format of the data product.

---

## 1.3 References

- Blazquez, A., Meyssignac, B., Lemoine, J.-M., Berthier, E., Ribes, A., Cazenave, A., Exploring the uncertainty in GRACE estimates of the mass redistributions at the Earth surface: implications for the global water and sea level budgets, *Geophysical Journal International*, 215 (1), 415–430, <https://doi.org/10.1093/gji/ggy293>, 2018.
- Caron, L., Ivins, E. R., Larour, E., Adhikari, S., Nilsson, J., and Blewitt, G.: GIA Model Statistics for GRACE Hydrology, Cryosphere, and Ocean Science, *Geophys. Res. Lett.*, 45, 2203–2212, <https://doi.org/10.1002/2017GL076644>, 2018.
- Carrère, L., and Lyard, F., Modeling the barotropic response of the global ocean to atmospheric wind and pressure forcing - comparisons with observations, *Geophys. Res. Lett.*, 30, 1275, doi:[10.1029/2002GL016473](https://doi.org/10.1029/2002GL016473), 6. 2003.
- Chen, J., Tapley, B., Seo, K.-W., Wilson, C., and Ries, J.: Improved Quantification of Global Mean Ocean Mass Change Using GRACE Satellite Gravimetry Measurements, *Geophys. Res. Lett.*, 46, 13984–13991, <https://doi.org/10.1029/2019GL085519>, 2019.
- Chen, J., Cazenave, A., Dahle, C., Llovel, W., Panet, I., Pfeffer, J., & Moreira, L.: Applications and challenges of GRACE and GRACE follow-on satellite gravimetry. *Surveys in Geophysics*, 1-41, 2022.
- Cheng, M., Tapley, B. D., and Ries, J. C.: Deceleration in the Earth's oblateness, *J. Geophys. Res.-Sol. Ea.*, 118, 740–747, <https://doi.org/10.1002/jgrb.50058>, 2013.
- Crétaux, J.-F., Abarca-del-Río, R., Bergé-Nguyen, M., Arsen, A., Drolon, V., Clos, G., and Maisongrande, P.: Lake Volume Monitoring from Space, *Surv. Geophys.*, 37, 269–305, <https://doi.org/10.1007/s10712-016-9362-6>, 2016.
- Dahle, C., Flechtner, F., Gruber, C., König, R., Michalak, G., & Neumayer, K.-H.: GFZ GRACE Level-2 Processing Standards Document for Level-2 Product Release 0005 : revised edition, January 2013. Scientific Technical Report STR - Data, Potsdam : Deutsches GeoForschungsZentrum GFZ, 21 p.. doi: 10.2312/GFZ.b103-1202-25, 2012.
- Dahle, C., Flechtner, F., Murböck, M., Michalak, G., Neumayer, H., Abrykosov, O., Reinhold, A. and König, R.: GRACE Geopotential GSM Coefficients GFZ RL06, V. 6.0, GFZ Data Services, [https://doi.org/10.5880/GFZ.GRACE\\_06\\_GSM](https://doi.org/10.5880/GFZ.GRACE_06_GSM), 2018.
- Decharme, B., Delire, C., Minvielle, M., Colin, J., Vergnes, J. P., Alias, A., ... & Voldoire, A.: Recent changes in the ISBA-CTRIP land surface system for use in the CNRM-CM6 climate model and in global off-line hydrological applications. *Journal of Advances in Modeling Earth Systems*, 11(5), 1207-1252, 2019.
- Dee, D. P., Uppala, S. M., Simmons, A. J., Berrisford, P., Poli, P., Kobayashi, S., ... & Vitart, F., The ERA-Interim reanalysis: Configuration and performance of the data assimilation system. *Quarterly Journal of the royal meteorological society*, 137(656), 553-597., 2011.
- Dobslaw, H., Bergmann-Wolf, I., Dill, R., Poropat, L., Thomas, M., Dahle, C., Esselborn, S., König, R., Flechtner, F., A new high-resolution model of non-tidal atmosphere and ocean mass variability for de-aliasing of satellite gravity observations: AOD1B RL06, *Geophysical Journal International*, 211 (1) 263–269. <https://doi.org/10.1093/gji/ggx302>, 2017.
- Frederikse, T., Riva, R. E. M., and King, M. A.: Ocean Bottom Deformation Due To Present-Day Mass Redistribution and Its Impact on Sea Level Observations, *Geophys. Res. Lett.*, 44, 12306–12314, <https://doi.org/10.1002/2017GL075419>, 2017.
- GRACE-FO; GRACEFO\_L2\_JPL\_MONTHLY\_0060. Ver. 6. PO.DAAC, CA, USA, Dataset accessed 2022-01-05 at <https://doi.org/10.5067/GFL20-MJ060>, 2019a.

- GRACE-FO; GRACEFO\_L2\_CSR\_MONTHLY\_0060. Ver. 6. PO.DAAC, CA, USA, Dataset accessed 2022-01-05 at <https://doi.org/10.5067/GFL20-MC060>, 2019b.
- Hugonnet, R., McNabb, R., Berthier, E., Menounos, B., Nuth, C., Girod, L., Farinotti, D., Huss, M., Dussailant, I., Brun, F., and Käab, A.: Accelerated global glacier mass loss in the early twenty-first century, *Nature*, 592, 726–731, <https://doi.org/10.1038/s41586-021-03436-z>, 2021.
- Kusche, J., Schmidt, R., Petrovic, S., and Rietbroek, R.: Decorrelated GRACE time-variable gravity solutions by GFZ, and their validation using a hydrological model, *J. Geodesy*, 83, 903–913, <https://doi.org/10.1007/s00190-009-0308-3>, 2009.
- Landerer, F. W., Flechtner, F. M., Save, H., Webb, F. H., Bandikova, T., Bertiger, W. I., ... & Yuan, D. N.: Extending the global mass change data record: GRACE Follow-On instrument and science data performance. *Geophysical Research Letters*, 47(12), e2020GL088306, 2020.
- Lemoine, J.-M., Bourgogne, S., Biancale, R., Bruinsma, S., and Gégout, P.: CNES/GRGS solutions Focus on the inversion process, in Paper presented at the GRACE Science Team Meeting, A1-02, Berlin, Germany, 2016.
- Lemoine J.-M., Reinquin F., Processing of SLR observations at CNES, *Newsletter EGS/EM*, October, Page 3. 2017.
- Lemoine, J. M., and Bourgogne, S.: RL05 monthly and 10-day gravity field solutions from CNES/GRGS (No. GSTM2020-51), Copernicus Meetings, 2020.
- Li, Y., Li, F., Shangguan, D., & Ding, Y.: A new global gridded glacier dataset based on the Randolph Glacier Inventory version 6.0. *Journal of Glaciology*, 67(264), 773-776. doi:10.1017/jog.2021.28, 2021.
- Loomis, B. D., Rachlin, K. E., and Luthcke, S. B.: Improved Earth Oblateness Rate Reveals Increased Ice Sheet Losses and Mass-Driven Sea Level Rise, *Geophys. Res. Lett.*, 46, 6910–6917, <https://doi.org/10.1029/2019GL082929>, 2019.
- Mayer-Gürr, T., Behzadpour, S., Ellmer, M., Kvas, A., Klinger, B., Strasser, S. and Zehentner, N.: ITSG-Grace2018 - Monthly, Daily and Static Gravity Field Solutions from GRACE, GFZ Data Services, <https://doi.org/10.5880/ICGEM.2018.003>, 2018.
- Peltier, W. R., Argus, D. F., and Drummond, R.: Comment on “An Assessment of the ICE-6G\_C (VM5a) Glacial Isostatic Adjustment Model” by Purcell et al., *J. Geophys. Res.-Sol. Ea.*, 123, 2019–2028, <https://doi.org/10.1002/2016JB013844>, 2018.
- Pfeffer, J., Cazenave, A., Blazquez, A., Decharme, B., Munier, S., & Barnoud, A.: Assessment of pluriannual and decadal changes in terrestrial water storage predicted by global hydrological models in comparison with GRACE satellite gravity mission, In revision for *Hydrol. Earth Syst. Sc.* 1–85. <https://doi.org/10.5194/egusphere-2022-1032>, 2023.
- RGI Consortium, 2017. Randolph Glacier Inventory - A Dataset of Global Glacier Outlines, Version 6. [Indicate subset used]. Boulder, Colorado USA. NSIDC: National Snow and Ice Data Center. doi: <https://doi.org/10.7265/4m1f-gd79>
- Scanlon, B. R., Zhang, Z., Save, H., Sun, A. Y., Müller Schmied, H., Van Beek, L. P., ... & Bierkens, M. F.: Global models underestimate large decadal declining and rising water storage trends relative to GRACE satellite data. *Proc. Nat. Ac. Sc.*, 115(6), E1080-E1089, 2018.
- Sun, Y., Riva, R., and Ditmar, P.: Optimizing estimates of annual variations and trends in geocenter motion and J2 from a combination of GRACE data and geophysical models, *J. Geophys. Res.-Sol. Ea.*, 121, 8352–8370, <https://doi.org/10.1002/2016JB013073>, 2016.
- Tang, L., Li, J., Chen, J., Wang, S.-Y., Wang, R., and Hu, X.: Seismic Impact of Large Earthquakes on Estimating Global Mean Ocean Mass Change from GRACE, *Remote Sens.*, 12, 935, <https://doi.org/10.3390/rs12060935>, 2020.
- Tapley, B. D., Bettadpur, S., Ries, J. C., Thompson, P. F., & Watkins, M. M.: GRACE measurements of mass variability in the Earth system. *science*, 305(5683), 503-505, 2004.

Uebbing, B., Kusche, J., Rietbroek, R., and Landerer, F. W.: Processing Choices Affect Ocean Mass Estimates From GRACE, *J. Geophys. Res.-Oceans*, 124, 1029–1044, <https://doi.org/10.1029/2018JC014341>, 2019.

Yuan D.-N.; GRACE Follow-On Level-2 Gravity Field Product User Handbook, JPL D-103922, [https://podaac-tools.jpl.nasa.gov/drive/files/allData/gracefo/docs/GRACE-FO\\_L2-UserHandbook\\_v1.0.pdf](https://podaac-tools.jpl.nasa.gov/drive/files/allData/gracefo/docs/GRACE-FO_L2-UserHandbook_v1.0.pdf), 2019.

## 1.4 Acronyms

Acronym	Description
CNES	Centre National d'Études Spatiales
CNRM	Centre National de Recherches Météorologiques
CSR	Center for Space Research
DEM	Digital Elevation Model
ECMWF	European Centre for Medium-Range Weather Forecasts
ERA-Interim	ECMWF Re-Analysis - Interim
EWH	Equivalent Water Height
GFZ	GeoForschungsZentrum
GIA	Glacial Isostatic Adjustment
GlaMBIE	Glacier Mass Balance Intercomparison Exercise
GPCC	Global Precipitation Climatology Center
GRACE	Gravity Recovery And Climate Experiment
GRACE-FO	Gravity Recovery And Climate Experiment- Follow On
ID	Identification
ITSG	Institute of Geodesy at Graz University of Technology
JPL	Jet Propulsion Laboratory
LEGOS	Laboratoire d'études en géophysique et océanographie spatiales
RGI	Randolph Glacier Inventory
ISBA-CTRIP	Interaction Soil Biosphere Atmosphere - CNRM version of Total Runoff Integrating Pathways
TUGRAZ	Technische Universität Graz
RMS	Root Mean Square
R&T	Recherche & Technologie
SLR	Satellite Laser Ranging
SURFEX	SURFace EXternalisée
TWS	Terrestrial Water Storage

**Table 1: List of acronyms.**



---

## 2 Study area and period

Time series of mass variations are provided for five RGI regions, namely the Arctic Canada North (RGI ID 3), Arctic Canada South (RGI ID 4), Iceland (RGI ID 6), Svalbard (RGI ID 7) and Russian Arctic (RGI ID 9) as shown in Figure 1 (surrounded by a red dotted line). The region outlines, provided by the RGI6 (RGI Consortium, 2017), have been discretized over a regular  $1^{\circ} \times 1^{\circ}$  grid. The area occupied by glaciers in each grid cell is estimated after Li et al., (2021). The glacier area in each region is calculated as the sum of glacier areas for all grid cells constituting the RGI regions. The glacier area in each region discretized over a regular  $1^{\circ} \times 1^{\circ}$  grid is consistent with the reference RGI 6.0 glacier area with a difference of less than 1% (Table 2).

All five regions have total surface areas (first column in Table 2) that are sufficiently large to be consistent with GRACE and GRACE-FO spatial resolution ( $\sim 100\,000\text{ km}^2$ ). We assume that the contribution of land hydrology is negligible with respect to the ice mass changes. As a consequence, even if glaciers occupy only a fraction of the total region area (third column in Table 2 after Li et al., 2021), the total mass changes over the full region area can be attributed to ice mass changes from glaciers. We explore the validity of this assumption in the section 4.2 Hydrological contribution. The contribution of hydrology is expected to be small with respect to glacier mass changes for Arctic islands, which is the main reason to limitate our study to these 5 regions.

Ice mass changes are provided for five RGI6 regions with an irregular time sampling from April 2002 to September 2022, corresponding to the GRACE and GRACE-FO era. The GRACE and GRACE-FO data are typically provided at a monthly time scale. However, several data gaps occur due to satellite operations (i.e. shorter than 4 months) and the time span (12 months) between the end of the GRACE mission (June 2017) and the beginning of the GRACE-FO mission (June 2018). Mass variations are estimated as the difference between two consecutive sampled months. As a consequence, there is no data gap in the dataset, but the time sampling is irregular.

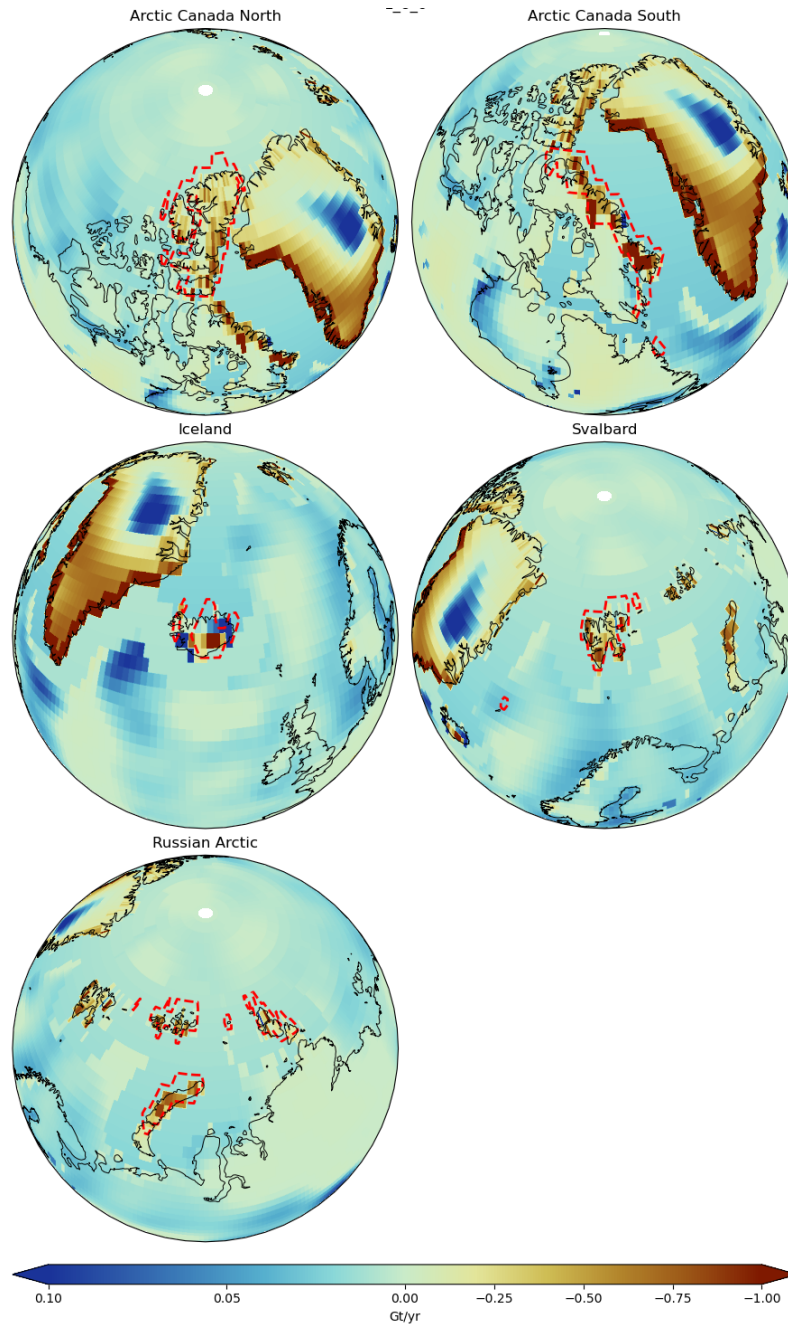


**Figure 1: Linear trends in surface mass anomalies calculated over April 2002- September 2022 based on GRACE and GRACE-FO measurements. The boundaries of RGI6 regions are shown in red.**

Region	Region area (km <sup>2</sup> )	Glacier area (km <sup>2</sup> )	Percentage of glacier area per region (%)	RGI6 reference glacier area (km <sup>2</sup> )	Difference in glacier area (km <sup>2</sup> )	Relative difference in glacier area (%)
Arctic Canada North	408 200	104 439	25.5	105 128	689	0.65
Arctic Canada South	324 914	40 673	12.5	40 888	215	0.52
Iceland	111 251	11 013	9.9	11 060	47	0.42
Svalbard	144 157	33 748	23.4	33 958	210	0.62
Russian Arctic	257 018	51 276	19.9	51 591	315	0.61

**Table 2: Surface areas of the five RGI6 regions considered in the present study. The glacier area in each region is taken after Li et al., 2021. The reference glacier area in each region is taken after the 6th RGI (RGI Consortium, 2017).**

## 3 Data and Methods

### 3.1 Overview

This section describes the methodology to compute the ice mass variations for the five selected RGI regions (Arctic Canada North, Arctic Canada South, Iceland, Svalbard, Russian Arctic) from satellite gravimetry measurements.

Section 3.2 describes the data and methodology used to estimate globally gridded surface mass anomalies, expressed as equivalent water heights (m), at a monthly time scale. An ensemble approach is adopted to robustly estimate the uncertainties associated with the processing and post-processing of satellite gravimetry data (Blazquez et al., 2018). An a priori based on DEM differencing data (Hugonnet et al., 2021) is used to reduce leakage errors and improve the accuracy of glacier mass balance estimates. An ensemble of 120

global monthly grids of surface mass anomalies is generated and expressed as equivalent water heights on a regular  $1^\circ \times 1^\circ$  grid on the WGS84 ellipsoid.

Section 3.3 describes the calculation of the regional mass balance for the 5 selected RGI regions (Arctic Canada North, Arctic Canada South, Iceland, Svalbard, Russian Arctic). For each of the 120 solutions of the ensemble, we calculate the total mass changes over each RGI region. The final estimate of the glacier mass balance is calculated as the ensemble mean of the 120 solutions for each region, with an uncertainty provided at 95% confidence interval based on the statistical distribution of the ensemble.

---

## 3.2 Global grids of surface mass anomalies

Gridded surface mass anomalies, expressed as equivalent water heights (m), have been estimated at global scale from April 2002 to September 2022 at a monthly temporal resolution and with a grid spacing of 1 degree using an ensemble of GRACE and GRACE-FO solutions. The GRACE and GRACE-FO ensemble is constituted of 120 solutions, allowing the estimation of uncertainties associated with different processing strategies and geophysical corrections needed for cryosphere applications.

The ensemble is based on the Earth's gravitational potential estimated by five different centers, expressed in Stokes coefficients (i.e. in the spherical harmonic basis) up to degree 96, including the JPL (RL06, GRACE-FO, 2019a; Yuan, 2019), CSR (RL06, GRACE-FO, 2019b; Yuan, 2019), GFZ (RL06, Dahle et al., 2018), ITSG (GRACE2018, Mayer-Gürr et al., 2018), and CNES-GRGS (RL05, Lemoine and Bourgoigne, 2020). However, such coefficients are affected by several sources of errors and limitations that need to be corrected in several post-processing steps.

- The GRACE and GRACE-FO satellites orbit around the center of mass, therefore are not sensitive to the geocenter motion, and cannot be used to evaluate the Stokes coefficients of degree 1. Two different models are used here to evaluate the geocenter motion (i.e. monthly values of the degree 1 coefficients by Sun et al., 2016 and Lemoine and Reinquin, 2017).
- The GRACE and GRACE-FO measurements are poorly sensitive to low degrees of the gravity field, in particular the  $C_{20}$  and  $C_{30}$  coefficients. Here, the  $C_{20}$  (full time series) and  $C_{30}$  (after May 2016 only) coefficients estimated by the five processing

centers are replaced by more robust SLR measurements from three different data centers (Cheng et al., 2013; Lemoine and Reinquin, 2017; Loomis et al., 2019).

- To extract mass variations due to present-day ice melting, GRACE and GRACE-FO data must be corrected for the ongoing deformations of the visco-elastic Earth due to the previous deglaciation. Two different GIA models are used here (Peltier et al., 2018, Caron et al., 2018). No little ice age (LIA) correction is performed.
- Stokes coefficients are affected by systematic correlated errors, easily identified in the spatial domain as characteristic stripes in the North-South direction. In order to reduce the anisotropic noise, decorrelation filters, called DDK filters (Kusche et al., 2009), are applied to GRACE solutions, using two different orders (DDK3 and DDK6) corresponding to two different levels of filtering.

The combination of five different processing centers, two geocenter models, three oblateness values ( $C_{20}$ ,  $C_{30}$ ), two GIA models and two levels of filtering leads to an ensemble of 120 solutions. Additional corrections are applied to all ensemble members in an identical way, related to de-aliasing background models and leakage errors.

The mitigation of leakage errors is critical for cryosphere applications. Leakage errors are associated with the mislocation of mass changes, due to the satellite configuration (i.e. limited spatial resolution, along-track correlations etc.) and inversion strategy (i.e. retrieval of the gravitational potential over a limited number of spherical harmonic coefficients leading to Gibbs oscillations). Leakage errors are propagated during the filtering step, which is necessary to extract statistically significant signals in a noisy solution. Leakage errors are particularly detrimental for cryosphere applications, as they result in an attenuation of the ice mass loss signal on the continents, leaking in the oceans (e.g. Chen et al., 2022).

To reduce leakage errors, the spherical harmonics solutions are separated in i) the a priori part including glacier mass changes from Hugonnet et al. (2021) data and lake mass changes from Crétaux et al. (2016) and ii) the residual part, which contains the signal to be filtered. The glaciological dataset evaluates glacier mass changes through the statistical analysis of DEM based on high-resolution satellite imagery, including the ASTER, SPOT5-HRS, SPOT 6-7, Pléiades, WorldView missions (see Hugonnet et al., 2021 for details). The hydrological dataset does not impact our glacier mass balance estimates as

no large lakes are located in the considered regions. The filter is therefore applied on smoother data, resulting in less signal loss around glaciers.

In addition, a leakage correction is applied on filtered residuals near the coast, displacing mass anomalies from the ocean to the near land. The leakage correction is based on the modeling of near-coast ocean as “region-wise” constant value for each time. In the final solutions, the a priori and the filtered residuals are added back together. The glacier mass changes from Hugonnet et al. (2021) are therefore not directly included in the GRACE data, as they are removed and added back after filtering, but they have a direct impact on the solution due to the non linearity of leakage correction and DDK filtering.

In the final solutions, ocean dealiasing models are restored using the GAB model from AOD1B RL06 (Dobslaw et al., 2017), except for the CNES solution using the TUGO model (Carrere and Lyard, 2003) during the GRACE period (2002-2016). Atmosphere dealiasing models are not restored. All centers use the GAA model from AOD1B RL06, except the CNES using ERA-Interim (Dee et al., 2011) during the GRACE period. The C0 coefficients are corrected to compensate for the total amount of water vapor in the atmosphere expressed in C0 GAA, in order to ensure the conservation of mass at global scale (Chen et al., 2019). This approach yields an ensemble of 120 solutions, consisting of monthly gridded surface mass anomalies, expressed as equivalent water heights over regular 1°x1° global grids (see Fig. 2).

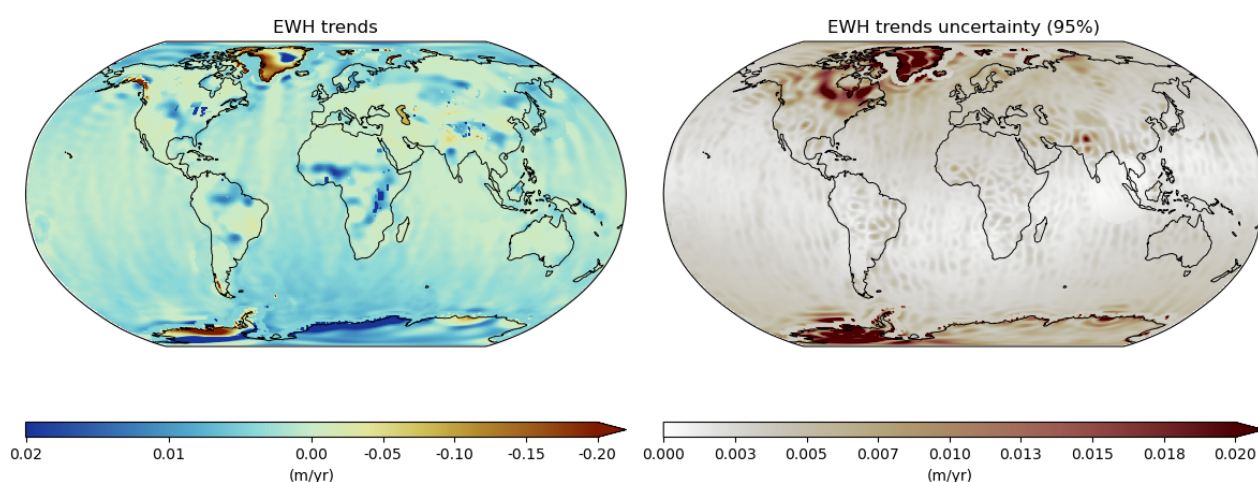


**Figure 2: Linear trends in surface mass anomalies over April 2002 - September 2022. a) Ensemble mean. b) Uncertainty with 95% confidence level derived from the covariance of the ensemble.**



### 3.3 Regional glacier mass balances

For each selected RGI 6.0 region  $R_i$  and each solution of the ensemble, the regional mass balance is calculated as:

$$M_{R_i}(t) = \rho_{water} \sum_{j=1}^n a_j \sigma_j(t) \quad (1)$$

where  $M_{R_i}(t)$  is the total mass anomaly at time  $t$  expressed in kg,  $\rho_{water}$  is the density of water taken as  $1000 \text{ kg m}^{-3}$  (i.e. the same density used to generate the grids in equivalent water height, cf. section 3.2.2),  $a_j$  are the surface areas of  $n$  individual grid cells constituting the  $R_i$  region expressed in  $\text{m}^2$  and  $\sigma_j(t)$  is the surface mass anomalies at time  $t$  within the  $j^{\text{th}}$  grid cell constituting the  $R_i$  region, expressed as equivalent water heights in m. The regional mass balances are then converted from kg to Gt, using a conversion factor of  $10^{-12}$ .

By applying this process to each of the 120 individual solutions of the GRACE and GRACE-FO ensemble, we obtain an ensemble of 120 glacier mass time series for each RGI region. Then, we compute the difference in mass between two consecutive times, thus obtaining an ensemble of 120 differentiated time series for each region. Finally, the mass balance over each RGI region is calculated as the mean of the 120 solutions of the ensemble. Assuming a normal distribution, the uncertainty at the 95% confidence interval on the glacier mass balance is calculated as the standard deviation of the ensemble multiplied by the corresponding critical value ( $C_{95\%} = 1.96$ ).

---

## 4 Results

### 4.1 Total mass changes of Arctic glaciers regions

Total mass changes have been estimated between April 2002 and September 2022 for five RGI 6.0 regions regrouping Arctic glaciers. The largest and smallest mass loss rates are observed over the Arctic Canada North (-38.0 +/- 1.7 Gt/yr) and Iceland (-7.8 +/- 0.5 Gt/yr) respectively, with significant annual (Table 3) and interannual variability (Figure 3).

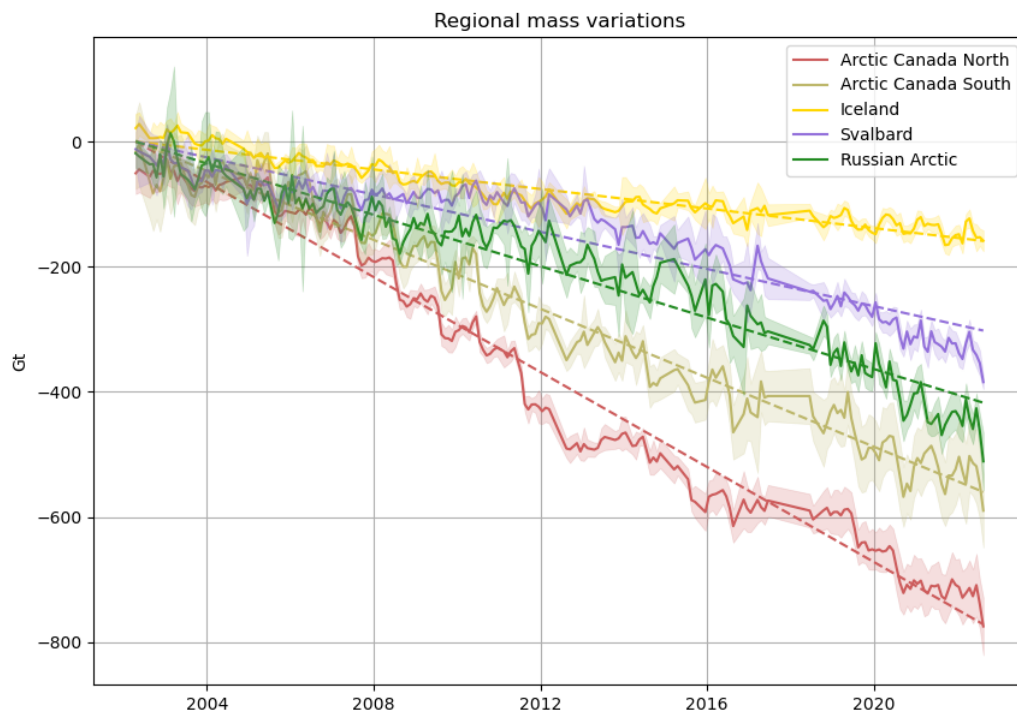


**Figure 3: Regional mass variations of Arctic glaciers from April 2002 to September 2022, 95% uncertainties.**

For each region, we have evaluated several metrics describing ice mass changes, including a linear trend, annual amplitude and phase and the residual root-mean square (RMS) of ice mass variations after removing a linear trend and annual sinusoid (Table 3).



Region	Trend (Gt/yr)	Annual amplitude (Gt)	Annual maximum (date)	Residual RMS (Gt)
Arctic Canada North	-37.9 +/- 3.4	13.2 +/- 2.8	19 April +/- 13 days	35.9 +/- 3.6
Arctic Canada South	-27.5 +/- 5.6	27.8 +/- 2.6	11 April +/- 18 days	23.8 +/- 1.7
Iceland	-7.8 +/- 1.0	10.5 +/- 3.6	08 April +/- 51 days	11.9 +/- 0.9
Svalbard	-14.9 +/- 1.3	6.3 +/- 5.6	08 April +/- 105 days	30.2 +/- 1.2
Russian Arctic	-20.5 +/- 1.8	16.4 +/- 11.0	15 February +/- 25 days	29.1 +/- 4.4

**Table 3: Characteristics of the total mass anomalies of Arctic glaciers regions over April 2002 - September 2022.**

We have presented here the total mass anomalies summed over each region, resulting in the time series displayed in Fig. 3. The dataset submitted to GLAMBIE contains the differences in total mass anomalies between two consecutively sampled months (see Eq. 3). The differentiation step tends to increase the noise in the time series because of the irregular time sampling of GRACE and GRACE-FO solutions and the high frequency noise in the gravimetry based estimates (see red line in Figure 4).

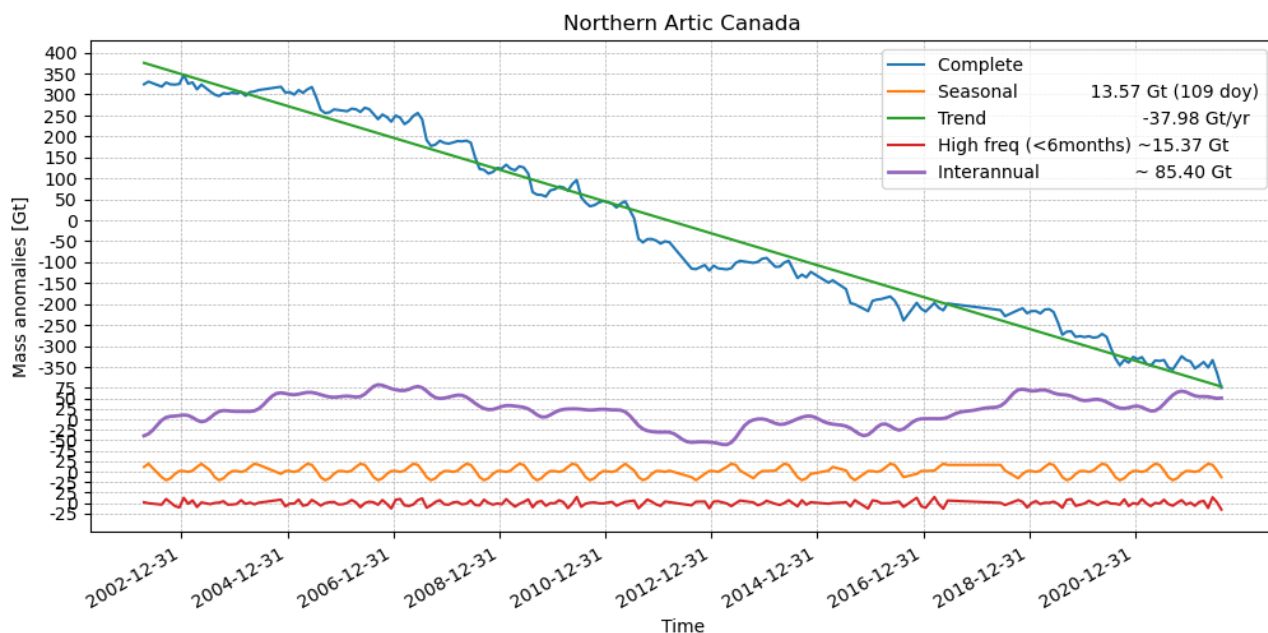


**Figure 4: Total mass anomalies (Gt) for the Arctic Canada North. The complete time series (blue) is analysed in terms of trend for the whole period (green), seasonal signal (yellow), high frequency for signals between 1 and 6 months (red) and interannual variability including signals over 1 year.**

The noise of this month to month mass change may be reduced by applying lowpass filters prior to the differentiation step (see for example figure 5). We decided not apply any lowpass filter in the submitted time series, to allow the reconstruction of the total mass anomalies at time  $t+1$ , as the cumulative sum of mass differences since time  $t$  as:

$$M_{Ri}(t + 1) = \sum_{t=0}^t \delta M_{Ri}(t) + M_{Ri}(t_0) \quad (2)$$

where:

$$\delta M_{Ri}(t) = M_{Ri}(t + 1) - M_{Ri}(t) \quad (3)$$

Because GRACE and GRACE-FO measurements only allow the estimation of mass anomalies,  $M_{Ri}(t_0)$  may be fixed to any arbitrary value such as 0. Generally, we recommend using the total mass anomalies  $M_{Ri}(t)$  rather than the total mass differences  $\delta M_{Ri}(t)$ , suffering from a higher level of noise and a less accurate description of errors (i.e. loss of information about correlated errors between two consecutive time steps).

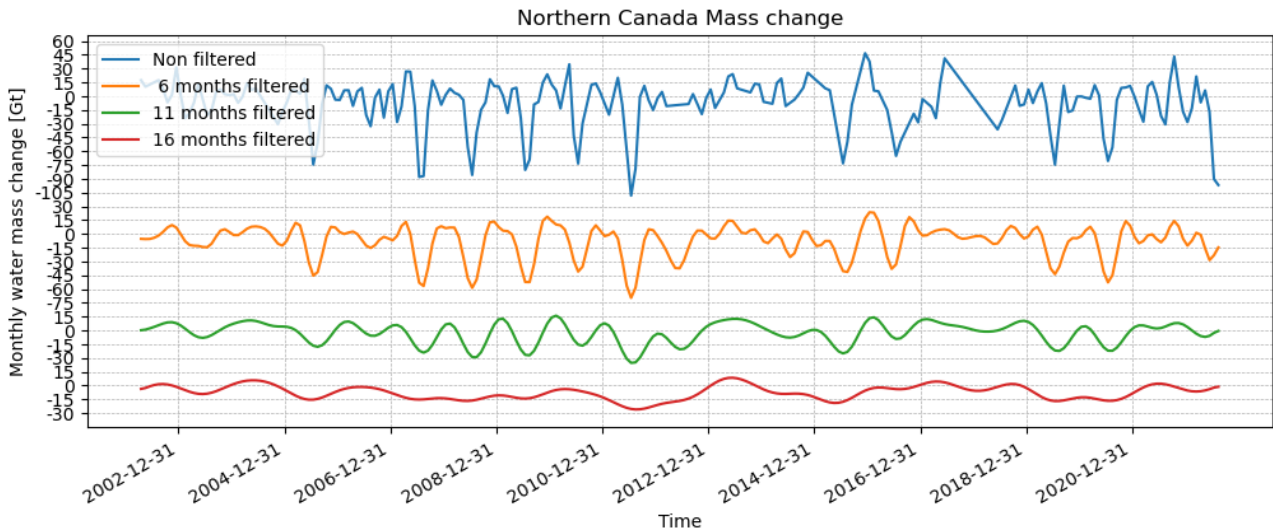


**Figure 5: Total mass anomalies (Gt) between two consecutively sampled months for the Arctic Canada North with and without application of a bandpass filter at 6, 11 and 16 months.**

## 4.2 Hydrological contribution

The contribution of land hydrology is assumed to be negligible in comparison with the ice mass changes of glaciers present in each region. We explore the validity of this assumption using the ISBA-CTRIP (Interaction Soil Biosphere Atmosphere - CNRM (Centre National de Recherches Météorologiques) version of Total Runoff Integrating Pathways) global land surface modeling system (Decharme et al., 2019).

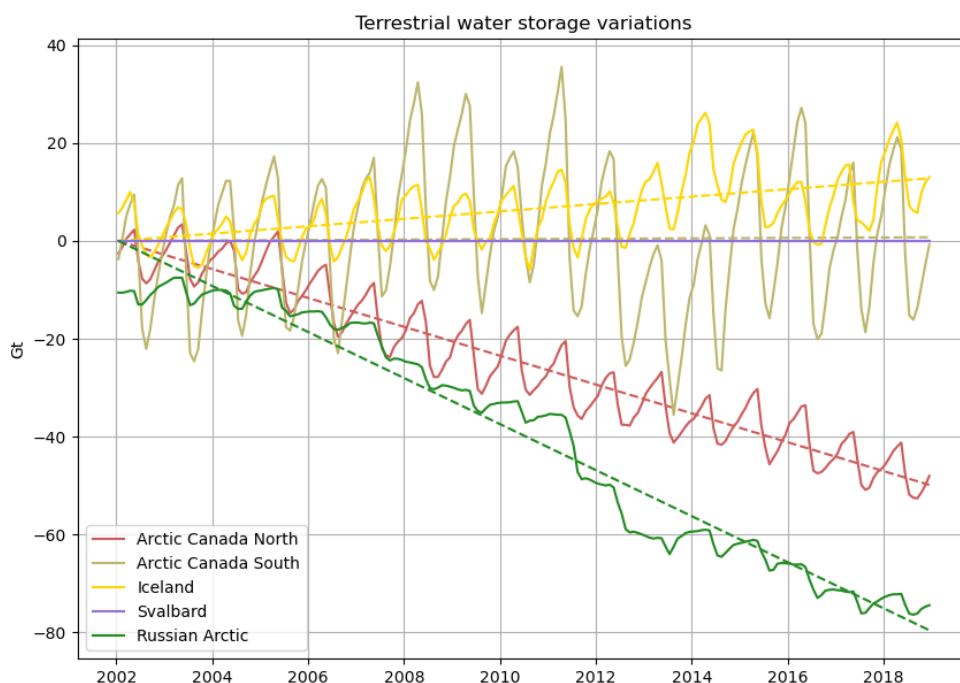


**Figure 6: Regional water mass variations of Arctic glaciers predicted by ISBA-CTRIP from April 2002 to December 2018.**

ISBA solves the water and energy balance in the soil, canopy, snow and surface water bodies, and CTRIP simulates discharges through the global river network, as well as the dynamic of seasonal floodplains and unconfined aquifers. ISBA and CTRIP are coupled through the land surface interface SURFEX (Surface Externalisée, in French), allowing interactions between the atmosphere, land surface, soil and aquifer. ISBA-CTRIP is forced with the ERA-Interim atmospheric reanalysis (Dee et al., 2011) for air temperature and humidity, wind speed, surface pressure and total radiative fluxes, and with the

gauge-based Global Precipitation Climatology Center (GPCC) Full Data Product V6 (Schneider et al., 2014) for precipitation.

RGI6 region	ISBA-CTRIP trend (Gt/yr)	ISBA-CTRIP residual RMS (Gt)	ISBA-CTRIP annual amplitude (Gt)	ISBA-CTRIP annual phase (°degrees)	GRACE trend over same period (Gt/yr)	Ratio of trends: ISBA-CTRIP to GRACE (%)
Arctic Canada North	-3.0	1.9	5.5	79.7	-27.5	10 %
Arctic Canada South	0.03	7.9	16.7	60.7	-22.1	0.1 %
Iceland	0.8	3.3	6.7	60.7	-6.3	12 %
Russian Arctic	-4.8	4.2	1.8	56.8	-11.6	41 %

**Table 4: Metrics for the terrestrial water storage variations (excluding glaciers) from ISBA-CTRIP hydrological model, for each of the RGI regions considered. The last column provides the percentage with respect to the total mass variations estimated in this study and provided in Table 3.**

The total terrestrial water storage (TWS) changes are calculated for each region, using the same formalism as for the ice mass changes (section 3.3, eq. 1), with  $\sigma_j(t)$  representing here the total TWS changes estimated with ISBA-CTRIP over April 2002 - December 2018 (limited before April 2002 by the availability of GRACE data and after December 2018 by the availability of the ISBA-CTRIP model). The TWS changes predicted from ISBA-CTRIP are then compared with the total mass changes from the GRACE and GRACE-FO ensemble over the same period (April 2002- December 2018) and regions (Arctic Canada North, Arctic Canada South, Svalbard, Iceland, Russian Arctic). For three out of the five regions, namely the Arctic Canada North, Arctic Canada South and Iceland, the contribution of land hydrology is small in comparison to the total mass changes estimated with the GRACE and GRACE-FO (i.e. ranging from 0.1% for the Arctic Canada South to 12% for Iceland). However, the contribution of land hydrology for the Russian Arctic (~ 41%) is significant with regard to total ice mass changes estimated with GRACE and GRACE-FO. Our total mass balance estimates must therefore be taken with careful consideration over the Russian Arctic, given that land hydrology may have a significant impact over this region. There are no hydrological predictions over the Svalbard region.

Large uncertainties affect hydrological models at decennial (e.g. Scanlon et al., 2018; Pfeffer et al., 2023) and interannual (e.g. Pfeffer et al., 2023) time-scales, especially over Arctic regions (e.g. Pfeffer et al., 2023; Decharme et al., 2019). Most global hydrological models, including ISBA-CTRIP, do not include glaciers in their modeling framework, leading to significant errors when predicting river discharge in glaciated regions (Decharme et al., 2019). It is therefore not recommended to use such hydrological models

in the vicinity of glaciers. We chose here to provide total mass changes over Arctic regions, without any correction applied for land hydrology, to avoid introducing the uncertainty inherent to hydrological model predictions on our glacier mass balance estimates. The analysis presented above using ISBA-CTRIP allows evaluating the limitations of this choice.

---

## 5 Product description

---

### 5.1 File specifications

#### 5.1.1 File format

The product is delivered as a set of CSV files. Metadata attributes are compliant with GLAMBIE submission requirements.

#### 5.1.2 File naming convention

The product follows the naming standard:

LEGOS-MAGELLIUM.V<VERSION>.RGI<RGI\_ID>.<RGI\_NAME>.csv

where:

- <VERSION> indicates the version of the dataset
- <RGI\_ID> indicates the RGI ID of the region described in the file
- <RGI\_NAME> indicates the RGI name of the region described in the file
- .csv is the standard CSV filename extension.

Example: LEGOS-MAGELLIUM.V1.6.0.RGI7.SVALBARD.csv is referring to the time series of total mass differences estimated over the Svalbard Region by the LEGOS-MAGELLIUM team.

### 5.1.3 Metadata

All metadata included in the csv is contained in the header.

## 5.2 Variables

The variables defined in the CSV files are the following:

Variables	Description	Units	Data Type
region_id	RGI region ID	no unit	int
start_date	start date of observation period	date in format DD/MM/YYYY	date
end_date	end date of observation period	date in format DD/MM/YYYY	date
glacier_change_observed	absolute change between start_date and end_date	Gt	float
glacier_change_uncertainty	uncertainty on the observed glacier change corresponding to 95% confidence interval.	Gt	float
unit	the units of "glacier_change_observed" and "glacier_change_uncertainty"	no unit	string
glacier_area_reference	regional glacier area (km <sup>2</sup> ) of reference dataset (i.e. RGI 6.0)	km <sup>2</sup>	float
glacier_area_observed	regional glacier area (km <sup>2</sup> ) covered by observations	km <sup>2</sup>	float
remarks	none	no unit	string
hydrological_correction_value	no correction	Gt	